RESEARCH ARTICLE

Isoconversional nonisothermal kinetic analysis of municipal solid waste, refuse-derived fuel, and coal

Mudassar Azam[1,2] (iD) | Asma Ashraf[2,3] | Saman Setoodeh Jahromy[1] | Waseem Raza[4] |
Hassan Khalid[2] | Nadeem Raza[5] | Franz Winter[1] (iD)

[1]Institute of Chemical, Environmental and Bio Science Engineering, TU WIEN, Vienna, Austria

[2]Institute of Chemical Engineering & Technology (ICET), University of the Punjab, Lahore, Pakistan

[3]Sharif College of Engineering & Technology, Affiliated with UET, Lahore, Pakistan

[4]State Key Laboratory of Fine Chemicals, Dalian University of Technology, Dalian, China

[5]Govt. Emerson College Affiliated with Bahauddin Zakaryia University, Multan, Pakistan

Correspondence
Mudassar Azam, Institute of Chemical, Environmental and Bio Science Engineering, TU WIEN, Vienna, Austria.
Email: mudassar.azam@tuwien.ac.at

Abstract

The thermal characteristics and kinetic behavior of various solid wastes, including refuse-derived fuel (RDF) and municipal solid waste (MSW), were investigated as a potential renewable energy source, in comparison with low-rank coal. The experimental data were obtained in nonisothermal conditions through TGA analysis at specific heating rates. In addition to thermal characteristics of solid fuels, four isoconversional (model-free) kinetic methods: a: Kissinger-Akahira-Sunose (KAS), b: Flynn-Wall-Ozawa (FWO), c: Friedman, and d: Vyazovkin were applied to calculate activation energies. In case of solid wastes, it is possible to say that the trend of activation energies of all isoconversional methods remains almost same in the selected region of conversion (0.1-0.6 and 0.7-0.9). Whereas in case of coal, Friedman model exhibits lower and inconsistent values of activation energy than others selected isoconversional methods. The experimental and modeling results revealed that that solid wastes (RDF and MSW) can be promising alternative energy sources to encounter energy crisis and uncontrolled waste disposal issues.

KEYWORDS

coal, isoconversional, model free, MSW, waste

1 | INTRODUCTION

The secure supply of energy sources is a key indicator for the sustainable development of societies. Normally, various types of fossil energy reserves (natural gas, coal, and gasoline) are the major sources of conventional energy demand. The use of fossil fuel for energy production is posing many problems including global warming, reduction in fossil energy sources, and other related environmental issues.[1,2] On the other hand, the population rise, economics, and rapid industrialization have also posed energy and environmental concerns in various countries.[3] It is estimated that about 1.2 billion people

globally still do not have even basic energy infrastructure.[4] At present, Pakistan is a developing country and facing serious energy crisis with total energy demand and supply of 93.91, 70.94 Mtoe, respectively.[5] Considering, the huge energy supply and demand gap, it is highly recommended to explore sustainable energy alternatives to address the issue of current energy crisis.

Coal is one of the abundantly and evenly distributed fossil fuel (~65% of the total fossil fuels) around the globe, unlike oil and gas reserves which are only present in a fewer regions of the world.[6] At present, coal is the major source of energy and continues to dominate as a main contributor for energy

generation in developing countries.[7] Pakistan has huge coal reserves that nearly approach to 185 billion tons in its different provinces, especially in Sindh. It is estimated that the recoverable coal reserves in Pakistan are about 1.45 thousand Mtoe with total production capacity of 2.33 Mtoe per year.[8] The continuous consumption of coal as an energy source can pose severe environmental concerns due to large amount of CO_2 emission in atmosphere.[9] Due to growing concerns of climate change and its associated environmental problems, authorities related to environmental protection are forcing to shift conventional energy sources to renewable energy sources to minimize carbon foot print.[2,10]

The generation, disposal, and treatment MSW are major concerns in every country. Currently, Pakistan is one of the developing countries, experiencing severe environmental issues that are mostly linked to mismanagement of MSW disposal. The continuous release of greenhouse gases (GHG) into the atmosphere due to inadequate landfills facilities ultimately results in serious environmental issues.[11] In Pakistan, the estimated release of methane into the atmosphere due to these unusual landfilling practices is about 14.18 Gg per year which contributes almost 22 times greater greenhouse effect than CO2.[12] In light of these concerns, energy from waste sources is getting much attraction worldwide. Currently, the most common and adopted strategies of waste disposals are landfilling, incineration, sea dumping, and composting.[13]

In the past few years, waste to energy concept in respective technology has gained great attention.[14,15] Incineration of waste is one of the simplest strategy to convert waste into its corresponding energy.[16] In this regard, a good understanding of the combustion process will be of great help in designing the incinerators with improved efficiency. The combustion process can be understood carefully by knowing the Kinetic parameters. The most popular and simple technique to study the combustion kinetic is thermogravimetric analysis (TGA). Many researchers have utilized the TGA analysis to evaluate kinetics of combustion process in incineration by developing various kinetic models.[17-22] Typically, two kinds of kinetic models are employed such as model-free (isoconversional) and model-fitting. In this paper, isoconversional methods were adopted, as these methods are reflected as more reliable and accurate compared to complex data fitting methods that are generally dependent to type of reaction mechanism and lead to imprecise data estimation over wide experimental range.[17,23,24] However, model-free strategy does not depend on a reaction mechanism for fitting of respective thermodynamic data that ultimately results in precise error-free modeling. Another significant issue is variation of activation energy during the combustion process, as combustion process consists of more than one steps with different activation energies. In model-fitting methods, whole combustion process is characterized by a single value of activation energy. Thus, value of activation energy obtained is an average value and cannot depict all the steps involved during combustion. Conversely, isoconversional models address this issue and estimate value of activation energy as function of fractional conversion (α) that varies continuously till the end of complete combustion.[25,26]

In this work, the thermogravimetric analysis is carried out, following by application of model-free methods to propose a set of the kinetic parameters for combustion of coal, MSW, and RDF, to provide fundamental information for optimization of combustion process. The novel objective was to investigate the variance in thermal decomposition and kinetic parameters of locally available sustainable fuels. The thermal behavior and kinetic data of MSW and RDF in comparison with coal with application of isoconversional are rare, it will help researchers and policymakers in great deal regarding planning of combustion and cocombustion of these fuels. The characteristics and thermogravimetric results of these samples used for evaluation of kinetics parameters are presented in our previous work.[27]

2 | MATERIALS AND METHODS

The preparation of experimental samples (MSW and RDF) was based on representative components of MSW collected from city Lahore, Punjab, Pakistan, as described in our previous paper,[28] whereas low-rank coal sample was taken from Chiragh reserves located in province of Punjab, Pakistan. Thermogravimetric analysis was performed with the sample size of 20 mg in Mettler Toledo (TGA/DSC 1 STAR, USA) System. Initially, samples were heated from room temperature to 105°C. Four specific heating rates (10, 20, 30, and 40°C/min) were adopted to reach final temperature of 1000°C. A holding time of 10 minutes and 30 minutes was insured at temperature of 105°C and 1000°C, respectively. Synthetic air with constant flow rate of 80 mL/min was provided for all complete runs of experiments.

3 | KINETIC MODELING

Generally, for solid particles the rate of reaction is given as follows:

$$\frac{d\alpha}{dt} = f(T) \times f(\alpha) \quad (1)$$

Here

$$f(T) = Ae^{-\frac{E}{RT}} \quad (2)$$

And α can be ascribed to fractional conversion and denoted as

$$\alpha = \frac{m_O - m_i}{m_O - m_\infty} \quad (3)$$

Further, $f(\alpha)$ can be denoted as a function of fractional conversion (α). The equation can be simplified in derivative form using Equation (2) at respective ramping rates for temperature increase.

$$\frac{d\alpha}{dT} = \frac{A}{\beta} e^{-\frac{E}{RT}} f(\alpha) \qquad (4)$$

3.1 | Isoconversional methods

Many researchers have pointed that the prediction of reaction kinetics with model-fitting approach always poses inaccurate estimation due to reaction mechanism involvement.[29-31] Conversely, isoconversional approach does not follow any preassumption for reaction mechanism that ultimately reduces the possibility of errors for homogenous and heterogeneous combustion kinetic data. This model-free approach can play an effective role to estimate activation energies in wide range of experimental temperatures and conversions. The isoconversional methods applied in this study are Flynn-Wall-Ozawa (FWO), Friedman, Kissinger-Akahira-Sunose (KAS), and Vyazovkin.

3.1.1 | Friedman differential model

Taking natural logarithm on Equation (4) will result in following form of equation

$$\ln\left[\beta_i\left(\frac{d\alpha}{dT}\right)_{\alpha,i}\right] = \ln\left[A_\alpha \times f(\alpha)\right] - \frac{E_\alpha}{RT_{\alpha,i}} \qquad (5)$$

Equation (5) present differential isoconversional model and is known as Friedman model. Many researchers have employed this approach for approximation of reaction kinetics in solid particles.[20,32-43]

E_α (apparent activation energy) can be calculated for respective conversion value (α) by estimating resultant slope of Equation (5) and $1/T_{\alpha,i}$.

3.1.2 | Vyazovkin integral model

This model-free approach is also known as nonlinear integral method that is outcome of revised expression of temperature integral from Equation (6).

$$g(\alpha) = \frac{A}{\beta} \int_0^T e^{-\frac{E}{RT}} dT \qquad (6)$$

$$g(\alpha) = \frac{A}{\beta_i} I\left(E_\alpha, T_{\alpha,i}\right) \qquad (7)$$

As for isoconversional models, $g(\alpha)$ is not dependent on heating rate so,

$$\frac{A_\alpha}{\beta_1} I\left(E_\alpha, T_{\alpha,1}\right) = \frac{A_\alpha}{\beta_2} I\left(E_\alpha, T_{\alpha,2}\right) = \ldots = \frac{A_\alpha}{\beta_n} I\left(E_\alpha, T_{\alpha,n}\right) \qquad (8)$$

The above equation can be rewritten as follows:

$$\sum_{i=a}^{n} \sum_{j \neq i}^{n} \left(\frac{I\left(E_\alpha, T_{\alpha,i}\right)}{\beta_i} \Big/ \frac{I\left(E_\alpha, T_{\alpha,j}\right)}{\beta_j}\right) = n(n-1) \qquad (9)$$

$$\left| n(n-1) - \sum_{i=a}^{n} \sum_{j \neq i}^{n} \left(\frac{I\left(E_\alpha, T_{\alpha,i}\right)}{\beta_i} \Big/ \frac{I\left(E_\alpha, T_{\alpha,j}\right)}{\beta_j}\right) \right| = \text{minimum} \qquad (10)$$

The integral value of $I(E_\alpha, T_{\alpha,i})$ can be evaluated by resolving a complex integration or by using Senum-Yang polynomial 4th-degree approximation[44] as described below.

$$p(x) = \exp\left(\frac{-x}{x}\right) \times \frac{x^3 + 18x^2 + 86x + 96}{x^4 + 20x^3 + 120x^2 + 240x + 120} \qquad (11)$$

x can be taken as equivalent to α in the previous equation. The activation energies can be calculated by substitution of experimental values (T_α and β) in Equation (10) with condition of changing E_α to approach a minimum value. The minimum value was achieved for each value of α to estimate activation energy dependency on conversion. This strategy has also been reported reliable and consistent in various studies reported in the literature.[25,31,32,36,40,45-47]

3.1.3 | Flynn-Wall-Ozawa method

This method was proposed by cumulative contribution of Flynn, Ozawa and Wall by the modification of Doyle contribution as described in Equation (12).

$$\ln(\beta_i) = \ln\left[\frac{A_\alpha E_\alpha}{Rg(\alpha)}\right] - 5.331 - 1.0516\frac{E_\alpha}{RT_{\alpha i}} \qquad (12)$$

The resultant straight lines by plotting Equation (12) vs $1/T_{\alpha i}$ will give the estimation of activation energy at different conversion levels.[35,37,38,45,48]

3.1.4 | Kissinger-Akahira-Sunnose method

$$\ln\frac{\beta_i}{T_{\alpha i}^2} = \ln\left[\frac{A_\alpha R}{E_\alpha g(\alpha)}\right] - \frac{E_\alpha}{RT_{\alpha i}} \qquad (13)$$

The resultant plot of Equation (13) vs $1/T_{\alpha i}$ yields slope equal to $-E_\alpha/R$. The application of this model has been reported satisfactory by many researchers.[41,49-52]

4 | RESULTS AND DISCUSSION

4.1 | TG and DTG profiles

TG and DTG curves for coal, MSW, and RDF were observed individually, as function of time and temperature range of 25°C to 1000°C. Figures 1 and 2 present TG and DTG trends of the sample fuels at specific heating rates (10, 20, 30, and 40°C/min). It is important to define the extent of conversion through an observable adequate physical property. According to different thermal decomposition studies, among all physical properties, mass loss is the most suitable physical property to describe the dependency of the overall rate constant on the temperature. The is mainly due to fact that the mass loss during the combustion process does not depend upon the heating rate.[53-56]

It is broadly accepted that fuel decomposition process mainly contains three stages over complete range of temperature, which are (a) moisture drying, (b) major loss of weight, due to release of volatile organic matter, and (c) consecutive slow combustion of fixed carbon.[57] Last two steps, certainly, are linked with chemical composition (homogeneous/heterogeneous nature) of these samples, as main constituent of

these samples has dissimilar degradation profiles, as shown in Figure 2. The physical composition of simulated solid wastes is presented in Table 1. The proximate and ultimate analysis presented in Table 2 showed that all the fuels were low in content of moisture and fixed carbon, as a result, first and third region showing less prominent weight loss. As expected, apart from the heating rate, the decomposition process of MSW and RDF shows a very high weight loss due to high reactivity, whereas coal TG behavior is slower, which is characterized by a low volatile content and high ash content. The mass percent of ash content of coal is ~32.1% that is much higher than that of MSW (~11.1%) and RDF (~12.9%). The decomposition pattern of solid wastes showed that a number of individual shoulders or peaks appeared at lower heating rate, which disappear or overlap as the heating rate is increased. The thermal decomposition of coal results in one major peak, due to release of carbon-containing volatile matter,[58] whereas existence of different peaks in case of solid wastes is credited to the heterogeneous nature of these wastes fuels. The solid wastes show prominent weight loss between 180°C and 550°C, whereas the coal weight loss is mainly between 400°C and 770°C at heating rate of 20°C/min. The solid wastes exhibit multicomponents sharp weight loss peaks in the fast devolatilization stage. The weight loss of first peak of MSW (~43.1%) and RDF (~39.8%) is mainly contributed by the highly volatile and easily decomposable components in solid wastes such as biodegradables (cellulose and hemicellulose), textile, and paper with temperature range
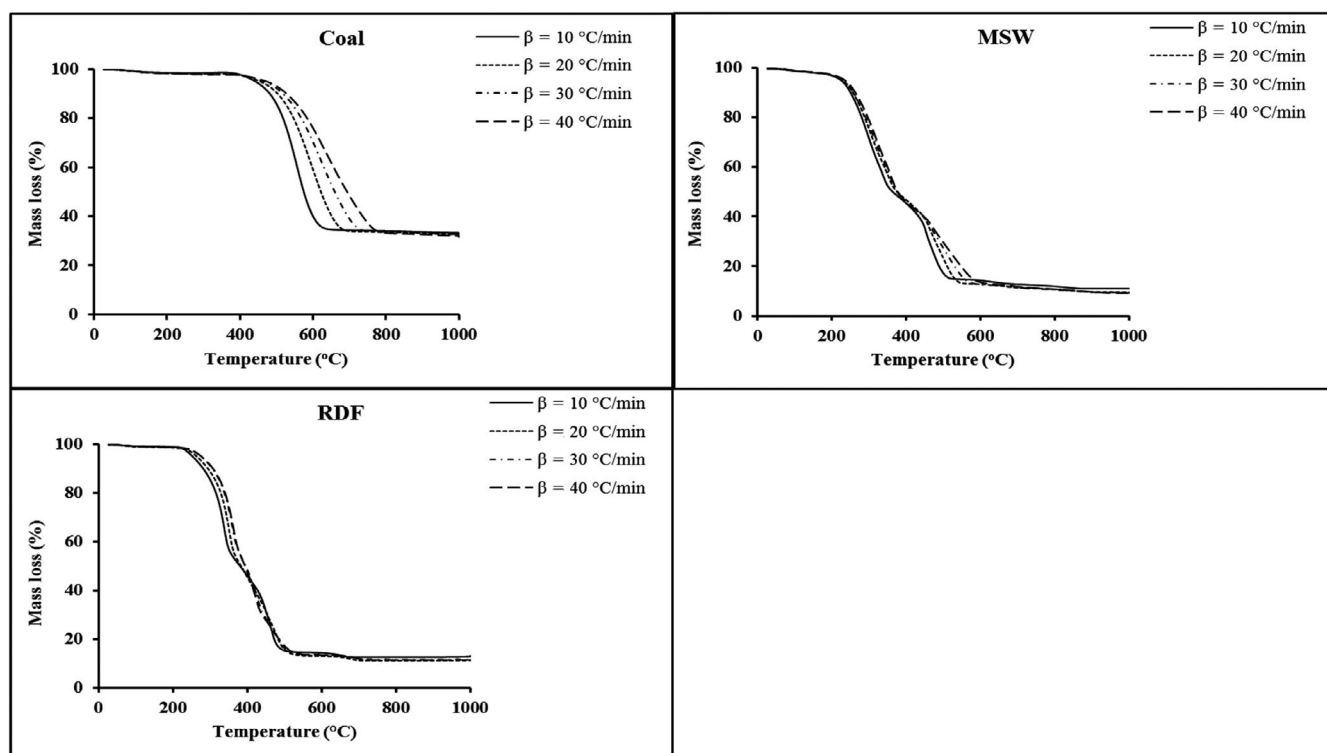

FIGURE 1 TG curves of coal, MSW, and RDF samples at different heating rates
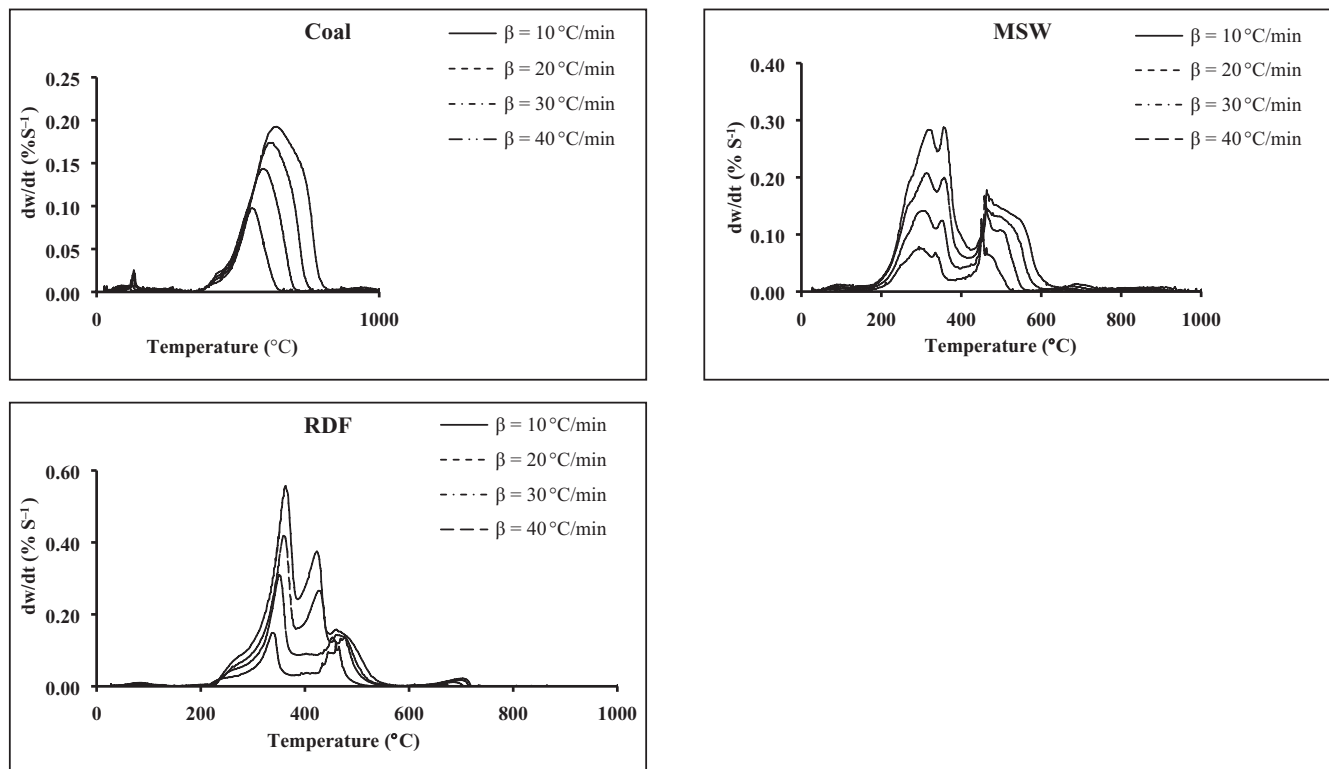
FIGURE 2 DTG curves of coal, MSW, and RDF at different heating rates

TABLE 1 Physical percentage (average) of MSW, simulated MSW, and simulated RDF[27]

Order	Material	True MSW (%)	Simulated MSW (%)	Simulated RDF (%)
1	Biodegradable	56	69	-
2	Nylon plastic bags	11	14.5	47.3
3	Textile	9.1	11.5	37.6
4	Paper	2.8	4.1	13
5	Noncombustible	6.3	-	-
6	PET	0.7	0.9	1.8
7	Tetrapak	1.1	-	-
8	Combustibles	6.2	-	-
9	Diaper	5.3	-	-
10	Hazardous	1.3	-	-
11	Glass	0.7	-	-

of 180-390°C and 216-376°C, respectively. The second volatile release peak from solid wastes mainly corresponds to combustion of mixed plastic (LDPE, HDPE, and PVC) with almost same temperature range 388-550°C for MSW and RDF. In the carbonization stage, tiny weight loss in MSW and coal is attributed to thermal decomposition of lignin and char present in samples. This result is in agreement with the findings of researchers using MSW and RDF as fuel samples in TGA.[16,17,59-61]

The combustion characteristic parameters such as the initial temperature, burnout temperature, and temperature at maximum weight loss obtained from TG and DTG curves for combustion of the studied samples at different heating rates are summarized in Table 3. Thermal behavior and characterization studies at specific heating rates are an imperative criterion for kinetics studies. It is noticed that the heating rate affects the TG and DTG curves.[62] At specific heating rates, contact of fuel particles varies, which change the curve shape and combustion characteristics considerably, as indicated in Figures 1 and 2. It is evident from analysis, with the increasing heating rates, TGA curves are shifted toward the right and DTG curves are slightly shifted toward higher

TABLE 2 Proximate & ultimate analysis of samples[27]

		Proximate analysis[a]				Ultimate analysis[b]					
Order	Samples	H_2O (%)	VM (%)	Ash (%)	F.C[c] (%)	C (%)	H (%)	O[c] (%)	N (%)	S (%)	HHV (kJ/kg)
1	Biodegradeable	4.1	77.5	10	8.4	62.5	8.0	28.8	0.4	0.1	10 338
2	Textile	2.94	81.23	5.01	10.82	58.4	4.98	35.7	0.6	0.16	20 392
3	Nylon plastic bags	0.02	93.71	5.52	0.741	78.7	12.4	8.7	0.12	0.02	40 416
4	Paper	3.44	75.85	18.82	1.89	50.5	6.41	42.3	0.22	0.55	16 239
5	PET bottles	ND	92.26	0.19	7.55	62.0	4.04	33.9	0.05	0.01	23 060
6	MSW	3.3	79.7	9.1	7.2	63.6	8.1	27.1	0.4	0.11	15 978
7	RDF	1.6	86.2	7.07	4.7	66.9	8.7	23.8	0.32	0.14	29 429
8	Coal	1.84	38.8	31.7	27.53	80.7	3.6	9.6	1.02	5.04	30 362

[a]Air-dried basis.

[b]Dried ash-free basis.

[c]Calculated by difference.

TABLE 3 The combustion characteristics parameters for Coal, MSW, and RDF from TG and DTG curves

Sample	Heating rate (°C/min)	T_i (°C)	T_f (°C)	T_1 (°C)	T_2 (°C)
Coal	10	443	713	562	-
	20	444	727	578	-
	30	451	743	599	-
	40	460	778	610	-
MSW	10	219	560	301	455
	20	223	573	313	461
	30	225	586	325	470
	40	230	598	329	479
RDF	10	238	556	316	465
	20	242	559	334	473
	30	245	563	342	481
	40	255	570	367	495

Note: T_i: the ignition temperature, T_f: burnout temperature, T_1, T_2: temperature at maximum weight loss rate of first peak and second peak.

peak temperatures without changing the thermal profile. This shows that the overall reaction rate in decomposition process is a function of temperature only.[55] Consequently, all the combustion characteristic parameters were shifted to higher values, showing thermal lag at increasing heating rate. This might be credited to heat and mass transfer limitations due to poor thermal conductivity of materials present in samples.[59] Among the selected fuel samples, coal has highest ignition and burnout temperature, while MSW and RDF have considerably low and slight close range of these temperatures. The coal ignition temperature at four heating rates (10, 20, 30, and 40°C/min) varies from 443°C to 460°C. For MSW and RDF, this thermal lag varies from 219°C to 230°C and 238°C to 255°C, respectively. Similar shift of temperature

zone/ thermal lag is observed for burnout temperature values. The higher burnout temperature of coal is attributed to higher ash content, which again is main factor for further characterization of burnout process. It is evident that the heating rate had a significant effect on the weight loss rate during combustion process. In combustion process of these samples, the higher heating rates result in lower weight loss (conversion) and high reactivity. The reactivity during combustion process is proportional to the height of DTG peak. In case of coal, as heating rate increased, the weight loss rate at same temperature is increased. As revealed in Figure 2, as heating rate increased from 10 to 40°C/min, the weight loss rate increased from to 0.1 to 0.19% S^{-1}. Even though, similar trend was observed in case of MSW and RDF, as greater weight loss rate was recorded in both peaks with increasing heating rate. However, in solid wastes overlapping of peaks was prominent at higher heating rates. This may be explained on the basis of residence time during the combustion process. At low heating rate, more residence time results in efficient and effective heat transfer compared to higher heating rate. Similar results of combustion process are reported by researcher using different heating rate such as MSW,[16,61] RDF,[17] and coal.[20] The reactivity of these fuels was investigated at peak temperatures, resulting an order of RDF > MSW > coal.

4.1.1 | Kinetic analysis

In order to describe the dependence of the activation energy (E_α) on the conversion degree, four models from model-free kinetic methods were tested. The isoconversional plots of KAS, FWO, and Friedman for conversion (α) range of 0.1-0.9 are shown in Figure 3. According to reported studies, the parallelism of these lines is accredited to the same reaction mechanism and kinetic behavior.[63] For considered range of
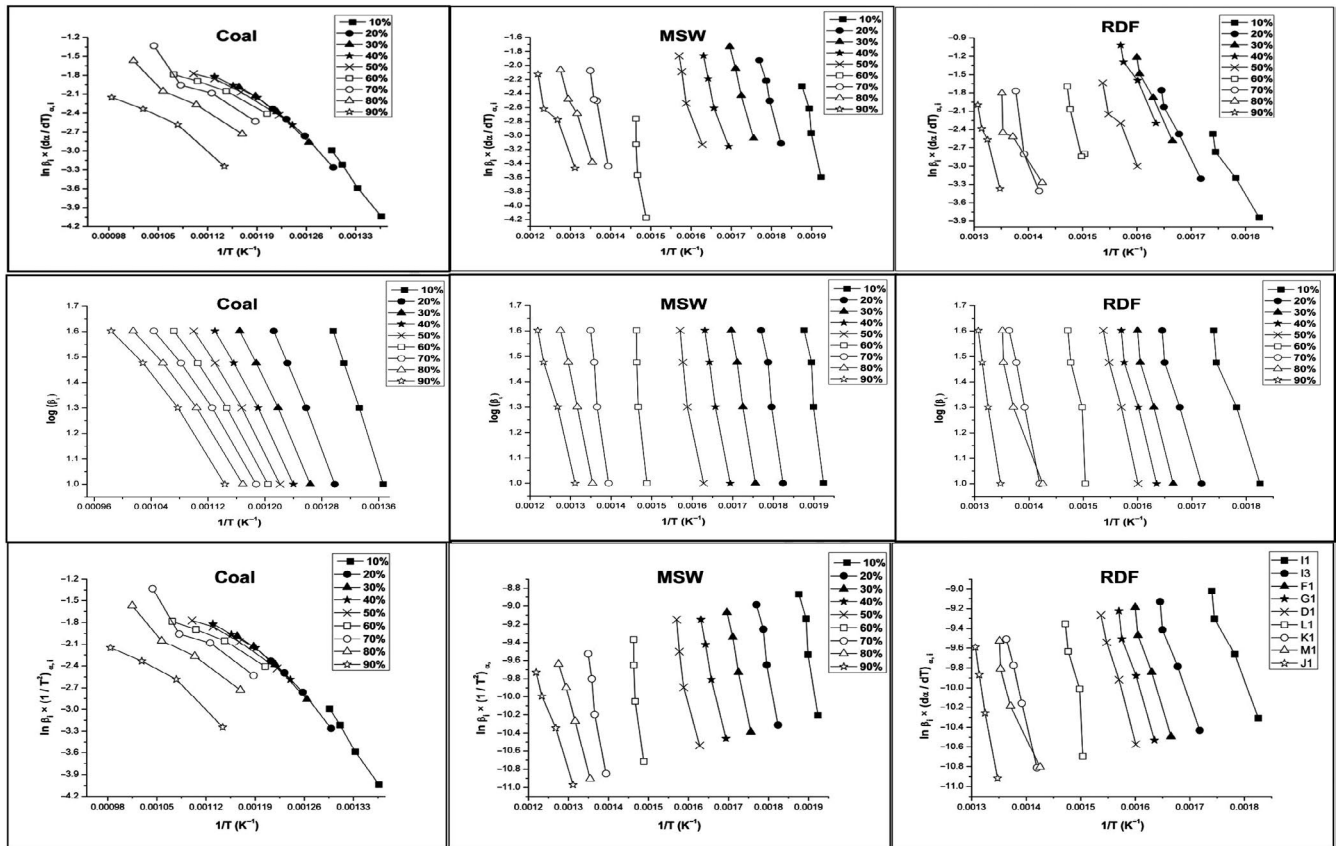
FIGURE 3 Plots for kinetic model. Friedman, FWO, KAS

conversion (α), the activation energy (E_α) values were obtained from individual slopes based upon linear model equations. The obtained E_α and correlation coefficient (R^2) values together with the values from nonlinear Vyazovkin procedure are summarized in Tables 4-6. The correlation coefficient of obtained E_α is close to unity, which indicates that these models had capability for better fit of experimental data

for estimation of kinetics. The average values of obtained E_α from isoconversional methods are summarized in Figure 4. Many researchers have presented such findings about isoconversional models.[17,25,29,32,64] Activation energy means the minimum energy requirement that must be acquired to start a reaction. This indicates, the reaction with high activation energy needs a high temperature or an extended reaction time.

TABLE 4 Dependency of activation energy (E_α, kJ/mol) of coal on conversion degree from model-free methods

	Coal						
	KAS		FWO		FM		VK
α	R^2	E_α	R^2	E_α	R^2	E_α	E_α
0.1	0.999	151.3	0.999	155.8	0.997	124	151
0.2	0.999	121.3	0.999	127.9	0.994	90.7	121
0.3	0.997	102.6	0.997	110.6	0.988	74.1	103
0.4	0.995	90.6	0.997	99.5	0.984	57.7	91
0.5	0.994	81.1	0.996	90.7	0.978	46.4	82
0.6	0.991	72.9	0.994	83.2	0.976	39.4	73
0.7	0.988	65.7	0.993	76.6	0.919	63.9	66
0.8	0.984	59.9	0.991	71.5	0.975	59.8	61
0.9	0.980	56.8	0.989	68.9	0.954	56.7	58
Average		89.2		98.3		68.1	89.5

TABLE 5 Dependency of activation energy (E_α, kJ/mol) of MSW on conversion degree from model-free methods

	MSW						
	KAS		FWO		FM		VK
α	R^2	E_α	R^2	E_α	R^2	E_α	E_α
0.1	0.954	239.9	0.957	236.5	0.968	232.1	240
0.2	0.980	210.3	0.981	208.8	0.992	186.1	210
0.3	0.997	186.5	0.997	186.5	0.996	184.1	186
0.4	0.991	172.9	0.992	173.9	0.969	168.2	173
0.5	0.952	179.1	0.957	180.2	0.941	175.1	179
0.6	0.873	376.2	0.879	368.5	0.822	379.9	205
0.7	0.973	243.2	0.976	242.8	0.980	245.2	243
0.8	0.998	134.4	0.999	139.8	0.986	134.1	134
0.9	0.993	108.4	0.995	115.6	0.933	108.5	109
Average		205.6		205.8		201.4	186.5

TABLE 6 Dependency of activation energy (E_α, kJ/mol) of RDF on conversion degree from model-free methods

	RDF						
	KAS		FWO		FM		VK
α	R^2	E_α	R^2	E_α	R^2	E_α	E_α
0.1	0.973	115.5	0.977	118.7	0.977	123.7	115
0.2	0.977	138.4	0.979	141.1	0.984	156.7	138
0.3	0.981	154.8	0.983	156.9	0.986	163.4	155
0.4	0.982	156.5	0.984	158.7	0.976	152.1	156
0.5	0.996	166.1	0.997	167.9	0.937	160.2	150
0.6	0.877	289.3	0.885	285.8	0.950	291.5	339
0.7	0.999	194.6	0.999	196.5	0.714	203.2	195
0.8	0.923	127.1	0.935	132.3	0.817	129.6	127
0.9	0.995	268.1	0.995	266.8	0.982	268.6	268
Average		178.9		180.5		183.2	182.5

Figures 5-7 show dependence of activation energy on the extent of selected fuel conversion. Comparison of obtained E_α showed that Vyazovkin, FWO, and KAS methods formed closer results than Friedman. The coal E_α at α 0.1 was found as 151.3, 155.8, 124, and 151 kJ/mol for each model as per given order in Table 4. For interval of α 0.2-0.9, the activation energies were close to each other with decreasing trend. This thermal event at temperature ~400°C and conversion degree ~0.1 is characterized by slow reaction rate with highest energy barrier ~155 kJ/mol, which means that in case of coal the energy requirement for the main mass combustion was less after initializing the reaction. It is noticeable that the coal activation energy values obtained from Friedman differential method are slightly lower than integral methods. In case of MSW and RDF, activation energy analysis shows tedious dependency on conversion and specifies the typical behavior of complex parallel reaction, involving multiple and consecutive degradation steps. For solid waste fuel, the changing

trend of E_α value obtained by these isoconversional methods is very consistent. The E_α values of solid wastes reported in the literature show great variation due to nonuniform composition of such kind of fuels. In case of solid wastes with the conversion rates increased from 0.1 to 0.9, two obvious peaks were observed at α: 0.1 and 0.6, respectively. As it can be observed from first peak of MSW, between $0.1 \leq \alpha \leq 0.5$ for temperature range between 180 and 365°C shows a progressive decrease in the activation energy from 239 to 180 kJ/mol, whereas first peak in case of RDF shows a progressive increase in the activation energy (118-165 kJ/mol) for same conversion degree with shorter temperature range between 226 and 356°C. This behavior is credited to complex multistep reaction during biomass decomposition of MSW. As mentioned earlier, the first peak is attributed to combustion of volatile matter and second peak corresponds to combustion of different organic compounds which offer greater energy barrier. Finally, both MSW and RDF at conversion degree 0.6 observed a maximum increase in activation energy values, ~365 kJ/mol and ~290 kJ/mol at corresponding temperature of 445°C and 405°C, respectively. This interval $0.6 \leq \alpha \leq 0.9$ is attributed to components of solid wastes with lower activity (biochar) and complex decomposition phase of PVC, which dictate the rate of reaction and need more energy under high temperature.[65,66] For solid wastes at conversion range ($\alpha = 0.1$-0.5), smaller fluctuations in E_α values with increasing trend were observed, whereas at conversion range ($\alpha = 0.6$-0.9), higher fluctuations with decreasing trend were observed throughout the process. This fluctuation in the E_α value is generally attributed to heterogeneous nature of solid wastes, which leads to complex reaction system including parallel, competitive, and complex reaction scheme.[57]

It is possible to say that the average activation energy of solid wastes obtained from all considered isoconversional methods is very close, compared to average activation energy of coal, as illustrated in Figure 7. It is important to note that the MSW E_α by the all isoconversional methods were
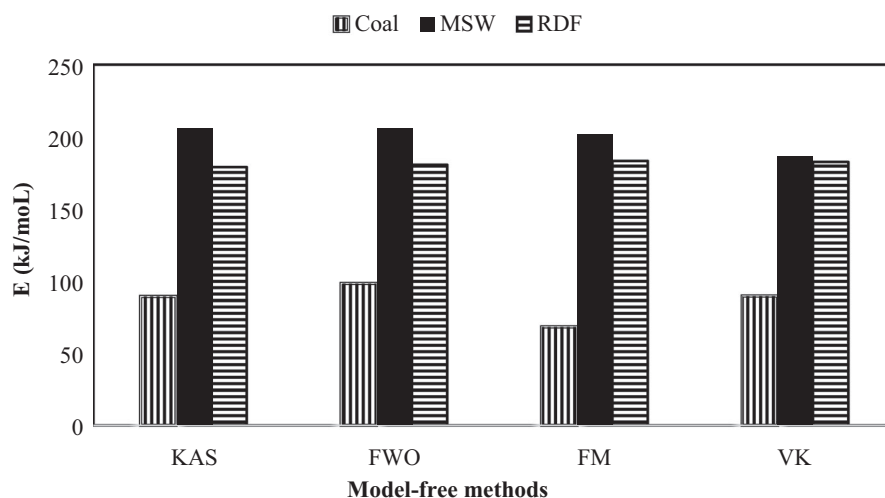
FIGURE 4 Average activation energy from model-free method

205.6, 205.8, 201.4, and 186.5 kJ/mol with the given order, which was 26.7, 25.3, 18.2, and 4.0 kJ/mol higher than that of RDF. This means, on average, more energy is required in the combustion process of MSW. It might be the result of less volatile content in MSW than RDF.[67] Conferring to kinetic analysis by all four isoconversional models, the selected fuels could be set in subsequent order of activation energy MSW > RDF > coal.
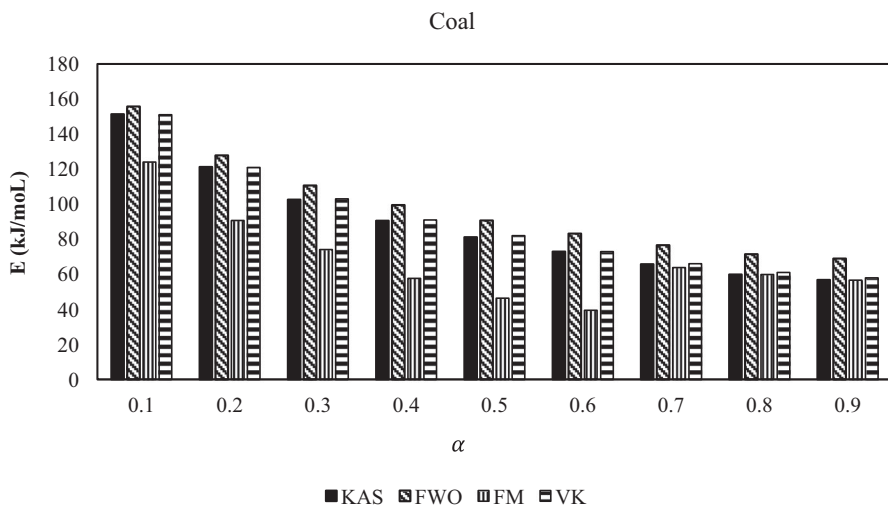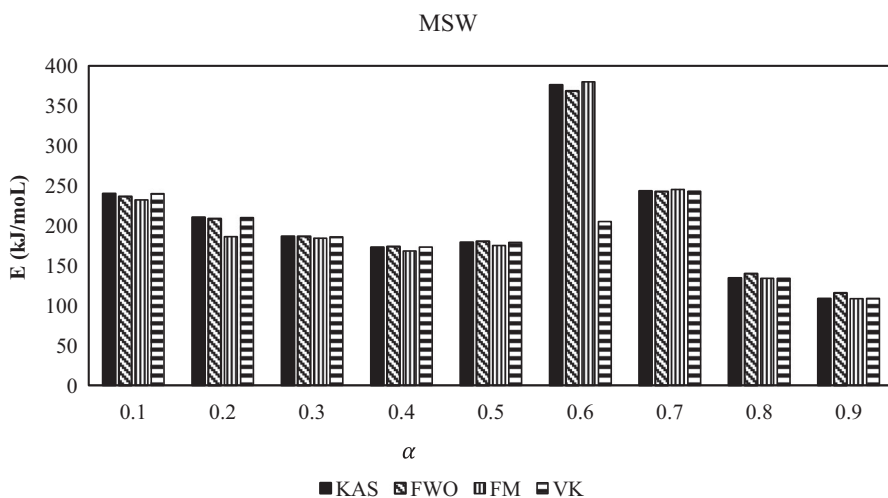

FIGURE 5 Activation energies based on coal conversion

FIGURE 6 Activation energies based on MSW conversion
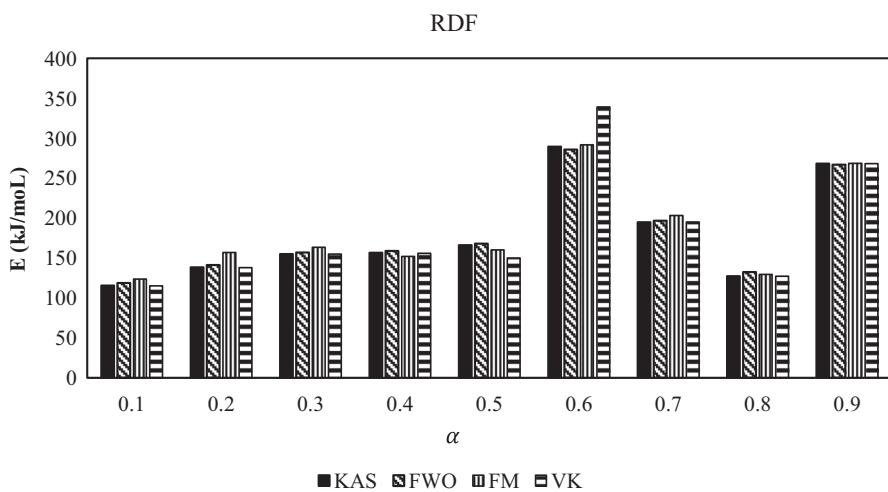
FIGURE 7 Activation energies based on RDF conversion

5 | CONCLUSION

According to TG and DTG analysis, it was observed that thermal decomposition of coal sample comprised single stage, whereas thermal decomposition of MSW and RDF involved complex set of multiple and simultaneous steps related to decomposition of biowaste (*ie,* food waste, textile, and paper) and plastic. The rate of thermal decomposition of all solid fuels was found increasing with the increase in heating rates. The dependency of the apparent activation energy (E_α) on conversion (α) was estimated through isoconversional approaches using three integral methods (Vyazovkin, KAS, and FWO) and one differential (Friedman) method. In case of coal, monotonic decrease in activation energy was found for selected conversion, whereas solid wastes observe two prominent peaks with conversion ranges between $0.1 \le \alpha \le 0.5$ and $0.6 \le \alpha \le 0.9$, with maximum activation energy value of MSW (~365 kJ/mol) and RDF (~290 kJ/mol) at conversion degree 0.6. The average activation energies were found as 89.2, 98.3, 68.1, and 89.5 kJ/mol for coal, 205.6, 205.8, 201.4, and 186.5 kJ/mol for MSW, and 178.9, 180.5, 183.2, and 182.5 kJ/mol for RDF using KAS, FWO, Friedman, and Vyazovkin approaches, respectively. In case of coal, it is worth noting that Friedman differential method exhibited lower values of for whole range of conversion.

The finding of this research work might open perspectives for the utilization (combustion and co-combustion) of solid wastes as promising alternative energy source and will provide new roadmap for waste management policies.

NOMENCLATURE

TGA	Thermogravimetric Analysis
MC	Moisture Content
FC	Fixed Carbon
RDF	Refuse Derived Fuel
HHV	High Heating Value
VM	Volatile Matter
MSW	Municipal Solid Waste
ad	air-dried basis
daf	dried ash-free basis
α	Fractional Conversion
E_α	Activation Energy (kJ/mol)
A	Pre-exponential Factor
β	Heating Rate (°C/min)
R	General Gas Constant
$f(\alpha)$	Differential Form of Reaction Model
$g(\alpha)$	Integral Form of Reaction Model
R^2	Correlation Coefficient
n	order of reaction

CONFLICT OF INTEREST

The authors have no potential conflicts of interest to declare.

ORCID

Mudassar Azam https://orcid.org/0000-0002-4557-2817
Franz Winter https://orcid.org/0000-0001-9854-3836

REFERENCES

1. Asif M, Muneer T. Energy supply, its demand and security issues for developed and emerging economies. *Renew Sustain Energy Rev*. 2007;11(7):1388-1413.
2. Raza W, Raza N, Agbe H, Kumar R, Kim K-H, Yang J. Multistep sequestration and storage of CO_2 to form valuable products using forsterite. *Energy*. 2018;155:865-873.
3. EIA. *International Energy Outlook 2017*. U.S.E.I. Administration, Editor; 2017. https://www.eia.gov/outlooks/ieo/pdf/0484(2017).pdf. Accessed January 01, 2020.
4. World Bank. *The Future of the World's Population in 4 Charts*. Worldbank.org; 2015. https://blogs.worldbank.org/opendata/future-world-s-population-4-charts. Accessed January 15, 2020.
5. IEA. *Pakistan: Indicators for 2015*; 2018. https://www.iea.org/statistics/statisticssearch/report/?year=2015&country=Pakistan&product=Indicators. Accessed July 23, 2018.
6. Fotovat F, Laviolette J-P, Chaouki J. The separation of the main combustible components of municipal solid waste through a dry step-wise process. *Powder Technol*. 2015;278:118-129.
7. Balat M. Coal in the global energy scene. *Energy Sources Part B*. 2009;5(1):50-62.
8. World Energy Council. *W. Energy Resources*; 2018. https://www.worldenergy.org/data/resources/country/pakistan. Accessed July 09, 2018.
9. Lohwasser R, Madlener R. Economics of CCS for coal plants: impact of investment costs and efficiency on market diffusion in Europe. *Energy Econ*. 2012;34(3):850-863.
10. Varol M, Atimtay A, Bay B, Olgun H. Investigation of co-combustion characteristics of low quality lignite coals and biomass with thermogravimetric analysis. *Thermochim Acta*. 2010;510(1-2):195-201.
11. Korai MS, Mahar RB, Uqaili MA. The feasibility of municipal solid waste for energy generation and its existing management practices in Pakistan. *Renew Sustain Energy Rev*. 2017;72:338-353.
12. Zuberi MJS, Ali SF. Greenhouse effect reduction by recovering energy from waste landfills in Pakistan. *Renew Sustain Energy Rev*. 2015;44:117-131.
13. Ionescu G, Rada EC, Ragazzi M, Mărculescu C, Badea A, Apostol T. Integrated municipal solid waste scenario model using advanced pretreatment and waste to energy processes. *Energy Convers Manage*. 2013;76:1083-1092.
14. Kantarelis E, Yang W, Blasiak W, Forsgren C, Zabaniotou A. Thermochemical treatment of E-waste from small household appliances using highly pre-heated nitrogen-thermogravimetric investigation and pyrolysis kinetics. *Appl Energy*. 2011;88(3):922-929.

15. Reina J, Velo E, Puigjaner L. Thermogravimetric study of the pyrolysis of waste wood. *Thermochim Acta*. 1998;320(1-2):161-167.

16. Liu G, Liao Y, Guo S, Ma X, Zeng C, Wu J. Thermal behavior and kinetics of municipal solid waste during pyrolysis and combustion process. *Appl Therm Eng*. 2016;98:400-408.

17. Çepelioğullar Ö, Haykırı-Açma H, Yaman S. Kinetic modelling of RDF pyrolysis: model-fitting and model-free approaches. *Waste Manage (Oxford)*. 2016;48:275-284.

18. Ren Q, Zhao C, Wu X, et al. TG–FTIR study on co-pyrolysis of municipal solid waste with biomass. *Biores Technol*. 2009;100(17):4054-4057.

19. Gai C, Dong Y, Zhang T. The kinetic analysis of the pyrolysis of agricultural residue under non-isothermal conditions. *Biores Technol*. 2013;127:298-305.

20. Ashraf A, Sattar H, Munir S. Thermal decomposition study and pyrolysis kinetics of coal and agricultural residues under non-isothermal conditions. *Fuel*. 2019;235:504-514.

21. Gao W, Chen K, Xiang Z, et al. Kinetic study on pyrolysis of tobacco residues from the cigarette industry. *Ind Crops Prod*. 2013;44:152-157.

22. Cai J, Liu R. Kinetic analysis of solid-state reactions: precision of the activation energy obtained from one type of integral methods without neglecting the low temperature end of the temperature integral. *Solid State Sci*. 2008;10(5):659-663.

23. Sergey Vyazovkin CAW. Model-free and model-ftting approaches to kinetic analysis of isothermal and nonisothermal data. *Thermochim Acta*. 1999;340–341:53-68.

24. Khawam A, Flanagan DR. Role of isoconversional methods in varying activation energies of solid-state kinetics. *Thermochim Acta*. 2005;436(1-2):101-112.

25. Brachi P, Miccio F, Miccio M, Ruoppolo G. Isoconversional kinetic analysis of olive pomace decomposition under torrefaction operating conditions. *Fuel Process Technol*. 2015;130:147-154.

26. Yorulmaz SY, Atimtay AT. Investigation of combustion kinetics of treated and untreated waste wood samples with thermogravimetric analysis. *Fuel Process Technol*. 2009;90(7-8):939-946.

27. Azam M, Jahromy SS, Raza W, Jordan C, Harasek M, Winter F. Comparison of the combustion characteristics and kinetic study of coal, municipal solid waste, and refuse-derived fuel: model-fitting methods. *Energy Sci Eng*. 2019;7(6):2646-2657.

28. Azam M, Jahromy SS, Raza W, et al. Status, characterization, and potential utilization of municipal solid waste as renewable energy source: Lahore case study in Pakistan. *Environ Int*. 2020;134:105291.

29. Burnham AK, Dinh L. A comparison of isoconversional and model-fitting approaches to kinetic parameter estimation and application predictions. *J Therm Anal Calorim*. 2007;89(2):479-490.

30. Burnham AK *Global Chemical Kinetics of Fossil Fuels. How to Model Maturation and Pyrolysis*. Springer International Publishing AG; 2017.

31. White JE, Catallo WJ, Legendre BL. Biomass pyrolysis kinetics: a comparative critical review with relevant agricultural residue case studies. *J Anal Appl Pyrol*. 2011;91(1):1-33.

32. Vyazovkin S, Burnham AK, Criado JM, Pérez-Maqueda LA, Popescu C, Sbirrazzuoli N. ICTAC Kinetics Committee recommendations for performing kinetic computations on thermal analysis data. *Thermochim Acta*. 2011;520(1-2):1-19.

33. Aboyade AO, Hugo TJ, Carrier M, et al. Non-isothermal kinetic analysis of the devolatilization of corn cobs and sugar cane bagasse in an inert atmosphere. *Thermochim Acta*. 2011;517(1-2):81-89.

34. Fasina O, Littlefield B. TG-FTIR analysis of pecan shells thermal decomposition. *Fuel Process Technol*. 2012;102:61-66.

35. Šimon P. Isoconversional methods. Fundamentals, meaning and application. *J Therm Anal Calorim*. 2004;76:10.

36. Farjas J, Roura P. Isoconversional analysis of solid state transformations. *J Therm Anal Calorim*. 2011;105(3):757-766.

37. Budrugeac P, Homentcovschi D, Segal E. Critical analysis of the isoconversional methods for evaluating the activation energy. I. Theoretical background. *J Therm Anal Calorim*. 2001;63:7.

38. Aboulkas A, El harfi K, El Bouadili A. Thermal degradation behaviors of polyethylene and polypropylene. Part I: pyrolysis kinetics and mechanisms. *Energy Convers Manage*. 2010;51(7):1363-1369.

39. Vyazovkin S, Sbirrazzuoli N. Isoconversional kinetic analysis of thermally stimulated processes in polymers. *Macromol Rapid Commun*. 2006;27(18):1515-1532.

40. Mishra RK, Mohanty K. Pyrolysis kinetics and thermal behavior of waste sawdust biomass using thermogravimetric analysis. *Bioresour Technol*. 2018;251:63-74.

41. Ceylan S. Kinetic analysis on the non-isothermal degradation of plum stone waste by thermogravimetric analysis and integral master-plots method. *Waste Manag Res*. 2015;33(4):345-352.

42. Chen C, Miao W, Zhou C, Wu H. Thermogravimetric pyrolysis kinetics of bamboo waste via Asymmetric Double Sigmoidal (Asym2sig) function deconvolution. *Bioresour Technol*. 2017;225:48-57.

43. Damartzis T, Vamvuka D, Sfakiotakis S, Zabaniotou A. Thermal degradation studies and kinetic modeling of cardoon (*Cynara cardunculus*) pyrolysis using thermogravimetric analysis (TGA). *Biores Technol*. 2011;102:6230-6238.

44. Senum GI, Yang RT. Rational approximations of the integral of the arrhenius function. *J Therm Anal*. 1977;11(3):445-447.

45. Vyazovkin S, Dollimore D. Linear and nonlinear procedures in isoconversional computations of the activation energy of nonisothermal reactions in solids. *J Chem Inf Model*. 1996;36:4.

46. Han Y. *Theoretical Study of Thermal Analysis Kinetics*. Mechanical Department, University of Kentucky; 2014.

47. Edreis EMA, Yao H. Kinetic thermal behaviour and evaluation of physical structure of sugar cane bagasse char during non-isothermal steam gasification. *J Mater Res Technol*. 2016;5(4):317-326.

48. Pahari G, Singh J, Parya TK. Non-isothermal decomposition kinetics of Cordierite precursor synthesized through semi-colloidal route from thermo-gravimetric data. *J Aust Ceram Soc*. 2016;52(2):11.

49. Ma Z, Chen D, Gu J, Bao B, Zhang Q. Determination of pyrolysis characteristics and kinetics of palm kernel shell using TGA–FTIR and model-free integral methods. *Energy Convers Manage*. 2015;89:251-259.

50. Mishra RK, Mohanty K. Pyrolysis characteristics and kinetic parameters assessment of three waste biomass. *J Renew Sustain Energy*. 2018;10(1):13102.

51. Radhakumari M, Prakash DJ, Satyavathi B. Pyrolysis characteristics and kinetics of algal biomass using tga analysis based on ICTAC recommendations. *Biomass Convers Biorefinery*. 2015;6(2):189-195.

52. Ceylan S, Topcu Y. Pyrolysis kinetics of hazelnut husk using thermogravimetric analysis. *Bioresour Technol*. 2014;156:182-188.

53. Aburto J, Moran M, Galano A, Torres-García E. Non-isothermal pyrolysis of pectin: a thermochemical and kinetic approach. *J Anal Appl Pyrol*. 2015;112:94-104.

54. Galano A, Aburto J, Sadhukhan J, Torres-García E. A combined theoretical-experimental investigation on the mechanism of lignin pyrolysis: role of heating rates and residence times. *J Anal Appl Pyrol*. 2017;128:208-216.

55. Lopez-Velazquez M, Santes V, Balmaseda J, Torres-Garcia E. Pyrolysis of orange waste: a thermo-kinetic study. *J Anal Appl Pyrol*. 2013;99:170-177.

56. Torres-García E, Ramírez-Verduzco L, Aburto J. Pyrolytic degradation of peanut shell: activation energy dependence on the conversion. *Waste Manage (Oxford)*. 2020;106:203-212.

57. Özsin G, Pütün AE. Kinetics and evolved gas analysis for pyrolysis of food processing wastes using TGA/MS/FT-IR. *Waste Manage (Oxford)*. 2017;64:315-326.

58. Idris SS, Rahman NA, Ismail K, Alias AB, Rashid ZA, Aris MJ. Investigation on thermochemical behaviour of low rank Malaysian coal, oil palm biomass and their blends during pyrolysis via thermogravimetric analysis (TGA). *Bioresour Technol*. 2010;101(12):4584-4592.

59. Ma Z, Wang J, Yang Y, et al. Comparison of the thermal degradation behaviors and kinetics of palm oil waste under nitrogen and air atmosphere in TGA-FTIR with a complementary use of model-free and model-fitting approaches. *J Anal Appl Pyrol*. 2018;134:12-24.

60. Ma Z, Sun Q, Ye J, Yao Q, Zhao C. Study on the thermal degradation behaviors and kinetics of alkali lignin for production of phenolic-rich bio-oil using TGA–FTIR and Py–GC/MS. *J Anal Appl Pyrol*. 2016;117:116-124.

61. Muthuraman M, Namioka T, Yoshikawa K. A comparative study on co-combustion performance of municipal solid waste and Indonesian coal with high ash Indian coal: a thermogravimetric analysis. *Fuel Process Technol*. 2010;91(5):550-558.

62. Leng Y. *Materials Characterization: Introduction to Microscopic and Spectroscopic Methods*. Chichester, UK: John Wiley & Sons (Asia) Pte Ltd; 2009.

63. Alvarenga L, Xavier T, Barrozo M, Bacelos M, Lira T. Analysis of reaction kinetics of carton packaging pyrolysis. *Procedia Eng*. 2012;42:113-122.

64. Hu S, Ma X, Lin Y, Yu Z, Fang S. Thermogravimetric analysis of the co-combustion of paper mill sludge and municipal solid waste. *Energy Convers Manage*. 2015;99:112-118.

65. Muthuraman M, Namioka T, Yoshikawa K. A comparison of co-combustion characteristics of coal with wood and hydrothermally treated municipal solid waste. *Biores Technol*. 2010;101(7):2477-2482.

66. Vamvuka D, Kakaras E, Kastanaki E, Grammelis P. Pyrolysis characteristics and kinetics of biomass residuals mixtures with lignite. *Fuel*. 2003;82(15-17):1949-1960.

67. Lin Y, Ma X, Yu Z, Cao Y. Investigation on thermochemical behavior of co-pyrolysis between oil-palm solid wastes and paper sludge. *Biores Technol*. 2014;166:444-450.